

Cyanide: A Strong-Field Ligand for Ferrohememes and Hemoproteins?*

Jianfeng Li, Richard L. Lord, Bruce C. Noll, Mu-Hyun Baik, Charles E. Schulz, and W. Robert Scheidt*

In memory of Gary Scheidt

Cyanide ion, a versatile diatomic ligand, has been extensively investigated as both a classic inhibitor and as a ligand for exploring properties of hemes and hemoproteins. Unlike CO and O₂, which bind only to iron(II) species, CN[−] can bind to both iron(II) and iron(III) hemoproteins. Stable low-spin (LS) iron(III) proteins can be straightforwardly prepared.^[1–3] In contrast, (cyano)iron(II) hemoproteins are usually indirectly formed by reduction of (cyano)iron(III) proteins. Cyanide-bound iron(II) forms of myoglobin,^[4] hemoglobin,^[5] horseradish peroxidase,^[6] and a number of cytochrome oxidase derivatives^[7] are known. Many, but not all, of the iron(II) species have lower binding constants than the iron(III) analogues. The equilibrium constant for cyanide binding for iron(III) hemoproteins is often greater than or equal to 10⁵ M^{−1}, compared to not more than 10² M^{−1} for iron(II) species.^[3]

Since we reported the first isolation of a (cyano)heme species in 1980,^[8] a number of electronic- and geometric-structure issues have been brought forward.^[9] All of the known species are LS iron(III) derivatives, either bis(cyano) [Fe^{III}(Por)(CN)₂][−] or mixed-ligand [Fe^{III}(Por)(CN)(L)] complexes (Por = porphyrin).^[9] However, there are no reported (cyano)iron(II) porphyrinate derivatives, presumably because this framework is known to have a lower stability and lower affinity for CN[−] than iron(III). It might be thought that (cyano)iron(II) species would be preferred, since a filled d⁶ shell should form strong π bonds to the π -accepting cyanide ligand.

We now report the first (cyano)iron(II) porphyrinate species, five-coordinate [K(222)][Fe(tpp)(CN)] (Figure 1, tpp = tetraphenylporphinato, 222 = Kryptofix 222). The average equatorial Fe–N_p bond length (1.986(7) Å) and the axial Fe–C bond length (1.8783(10) Å) are consistent with a

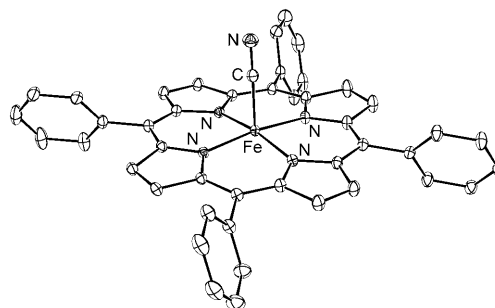


Figure 1. 100 K ORTEP diagram of [Fe(tpp)(CN)][−]. Thermal ellipsoids are set at the 50% probability level. Hydrogen atoms omitted for clarity.

LS state.^[10] However, temperature-dependent Mössbauer spectra reveal a more complicated picture of the iron spin state. A single quadrupole doublet is observed, whose value decreases from 1.827 mm s^{−1} at 25 K to 0.85 mm s^{−1} at 300 K; the isomer shift varies between 0.37 to 0.47 mm s^{−1}. The most probable explanation for these data is that a thermally induced spin crossover is occurring, and that interconversion between the two spin states is rapid on the Mössbauer time scale (less than 10^{−8} s).^[11a] This interpretation has been confirmed by both DFT calculations and magnetic susceptibility measurements.

The magnetic susceptibility of [K(222)][Fe(tpp)(CN)] was investigated over the temperature range of 2–400 K. Figure 2 shows the product of the molar susceptibility (χ_M ; corrected for temperature-independent paramagnetism (TIP)) and temperature (T) in an external magnetic field of 2 T, which provides direct evidence for an $S = 0$ (LS) \leftrightarrow $S = 2$ (high-spin,

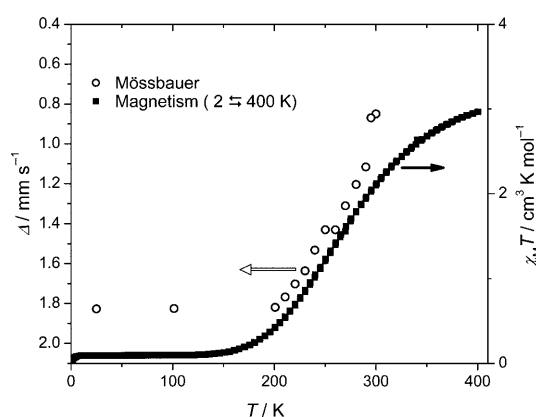


Figure 2. $\chi_M T$ versus T for [K(222)][Fe(tpp)(CN)] at 2 T applied field. The Mössbauer quadrupole splitting values are also presented for comparison.

[*] Dr. J. Li, Dr. B. C. Noll, Prof. W. R. Scheidt
Department of Chemistry and Biochemistry
University of Notre Dame, Notre Dame, Indiana 46556 (USA)
Fax: (+1) (574) 631-6652
E-mail: Scheidt.1@nd.edu

R. L. Lord, Prof. M.-H. Baik
Department of Chemistry, Indiana University (USA)
Prof. C. E. Schulz
Department of Physics, Knox College (USA)

[**] We thank the National Institutes of Health for support of this research under Grant GM-38401 to W.R.S. and the NSF for X-ray instrumentation (Grant CHE-0443233).

Supporting information for this article is available on the WWW under <http://dx.doi.org/10.1002/ange.200804116>.

HS) spin crossover. At 400 K, the value of $\chi_{\text{M}}T$ ($2.96 \text{ cm}^3 \text{ K mol}^{-1}$) is close to that expected for the HS state, but the lack of a significant plateau suggests that the transition is not quite complete at this temperature. The spin-state transition occurs over a large temperature range (ca. 175–400 K) and is reversible; both ascending and descending temperature measurements are shown in Figure 2, and no hysteresis was observed. The transition temperature $T_{1/2}$ (defined as temperature at which complexes show a population of 50 % in the HS state) of this gradually proceeding spin transition is about 265 K. Figure 2 also plots the observed time-averaged quadrupole splitting value against temperature; the strong correlation between the quadrupole splitting and the susceptibility is clear.

To gain a better understanding of the thermodynamic behavior of the spin states, density functional theory was employed (see the Supporting Information).^[12] At low temperature, only the low-spin $S = 0$ state was thermodynamically accessible. With increasing temperature the $S = 2$ state became significant, and a spin-crossover event is predicted to occur near 325 K (Figure S1 in the Supporting Information), in good agreement with the value of 265 K from experiment. The intermediate-spin $S = 1$ state was disfavored over the entire temperature range explored.

We have also investigated the temperature-dependent structure of the iron complex, as changes in metal–donor separations, along with changes in magnetic properties, are a hallmark of spin-state transitions. Structures were determined at 100 K (two crystals) and at 296, 325, and 400 K.^[13] A change from a LS to a HS state in the five-coordinate complex is expected to lead to increases in the axial Fe–C separation, the equatorial Fe–N_p bond lengths, and the displacement of the iron atom from the mean porphyrin plane. The results are summarized in the ORTEP drawings given in Figure 3; for simplicity only the cyanide group and FeN₄ porphyrin core are shown. The Fe–C bond elongates by 0.23 Å (Figure 3), which is amongst the largest changes in bond lengths that have been observed for iron(II) spin-crossover compounds.^[11b] This change takes place in part because the axial and equatorial bond-length increases must be asymmetric owing to the macrocyclic constraints of the porphyrin ring; note that Fe–N_p bond length has increased by 0.103 Å over the same temperature range. The average Fe–N_p bond length at 100 K (1.986 (7) Å) is that for a pure LS state, whereas the 400 K value (2.089 (8) Å) is slightly less than expected for an anionic HS iron(II) complex, consistent with the idea that the spin-

state transition is not quite complete. Also completely consonant with expectation are the increases in the displacement of the iron center from the mean plane of the four nitrogen plane.

The anisotropic thermal parameters also show evidence of the spin crossover. As expected, the magnitude of all atomic anisotropic displacement parameters increases with increasing temperature. However, the cyanide carbon atom shows different behavior over the temperature range. The thermal parameters at 100 and 400 K are close to isotropic, consistent with a single carbon atom site, whereas at intermediate temperatures with substantial populations of two spin states and differing carbon sites, the thermal parameters are much more prolate, with elongation along the Fe–C bond direction. Importantly, the C–N bond length in all structures remains nearly constant, as expected if only CN[−] atoms occupy two sites.

Additional evidence for the spin crossover comes from temperature-dependent IR spectroscopy, which has the advantage of a shorter time scale (10^{-13} s) and thus can detect both spin isomers. Measurements at 296 K, as either nujol mulls or KBr pellets, show two distinct $\nu(\text{C–N})$ frequencies at 2070 and 2105 cm^{-1} , with the first being stronger (see the Supporting Information). On cooling, the 2105 cm^{-1} peak gradually decreases in intensity, while the 2070 cm^{-1} peak increases in intensity. At 150–160 K, the stretch at 2105 cm^{-1} disappears, and thus it can be assigned to the HS stretch. A similar pattern of temperature-dependent azide stretches was observed in a 5/2–3/2 spin-crossover complex.^[14]

In coordination chemistry, cyanide and CO are deeply entrenched as strong-field ligands.^[15,16] Recently, Miller and co-workers showed that $[(\text{NEt}_4)_3][\text{Cr}^{\text{II}}(\text{CN})_5]$ ^[17] is a distorted trigonal bipyramidal complex that is not low-spin. Two different theoretical calculations^[18] suggested that the HS state results from the buildup of electrostatic (ligand–ligand) repulsions and not from the ligand field of cyanide per se; the cyanide ligand is behaving as a strong-field ligand in this chromium complex. However, $[\text{K}(222)][\text{Fe}(\text{tpp})(\text{CN})]$ represents a case in which the CN[−] ligand should unequivocally lead to LS species. That it does not strongly demonstrates the weaker-field nature of cyanide, even in a case where π back-bonding should be maximized.

In summary, the synthesis and characterization of the first cyanoiron(II) porphyrinate, $[\text{K}(222)][\text{Fe}(\text{tpp})(\text{CN})]$, is presented. It forms a LS-to-HS crossover complex; coordination of a single axial cyanide ligand does not generate a sufficiently strong ligand field to ensure a low-spin complex under all conditions.^[19] This finding is in distinct contrast to the analogous five-coordinate CO complex, which is low-spin under all known conditions.

Received: August 21, 2008

Published online: November 6, 2008

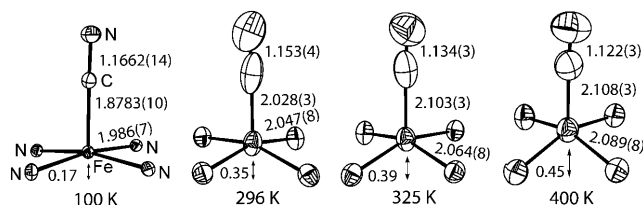


Figure 3. ORTEP diagrams of the core porphyrin atoms (Fe and four pyrrole N atoms) and the cyanide groups of $[\text{K}(222)][\text{Fe}(\text{tpp})(\text{CN})]$ at different temperatures. Axial ligand and average equatorial bond lengths are given as well as the iron displacement from the mean N₄ plane. Thermal ellipsoids are set at the 50% probability level.

Keywords: cyanides · iron · magnetic properties · porphyrinoids · spin crossover

- [1] E. Antonini, M. Brunori, *Hemoglobin and Myoglobin in Their Reactions with Ligands*, North-Holland, Amsterdam, **1971**.
- [2] D. Keilin, E. F. Hartree, *Biochem. J.* **1951**, *49*, 88.
- [3] M. Milani, Y. Ouellet, H. Ouellet, M. Guertin, A. Boffi, G. Antonini, A. Bocedi, M. Mattu, M. Bolognesi, P. Ascenzi, *Biochemistry* **2004**, *43*, 5213.
- [4] K. S. Reddy, T. Yonetani, A. Tsuneshige, B. Chance, B. Kushkuley, S. S. Stavrov, J. M. Vanderkooi, *Biochemistry* **1996**, *35*, 5562.
- [5] a) A. Boffi, A. Ilari, C. Spagnuolo, E. Chiancone, *Biochemistry* **1996**, *35*, 8068; b) A. Boffi, E. Chiancone, E. S. Peterson, J. Wang, D. L. Rousseau, J. M. Friedman, *Biochemistry* **1997**, *36*, 4510.
- [6] a) G. Rakshit, T. G. Spiro, *Biochemistry* **1974**, *13*, 5317; b) J. Teraoka, T. Kitagawa, *Biochem. Biophys. Res. Commun.* **1980**, *93*, 694; c) S. Yoshikawa, D. H. O'Keeffe, W. S. Caughey, *J. Biol. Chem.* **1985**, *260*, 3518; d) B. Meunier, J. N. Rodriguez-Lopez, A. T. Smith, R. N. F. Thorneley, P. R. Rich, *Biochemistry* **1995**, *34*, 14687.
- [7] a) W. S. Caughey, A. Dong, V. Sampath, S. Yoshikawa, X.-J. Zhao, *J. Bioenerg. Biomembr.* **1993**, *25*, 81; b) S. Yoshikawa, M. Mochizuki, X.-J. Zhao, W. S. Caughey, *J. Biol. Chem.* **1995**, *270*, 4270; c) Y. Kim, G. T. Babcock, K. K. Surerus, J. A. Fee, R. B. Dyer, W. H. Woodruff, W. A. Oertling, *Biospectroscopy* **1998**, *4*, 1; d) A. Jafferji, J. W. A. Allen, S. J. Ferguson, V. Fülöp, *J. Biol. Chem.* **2000**, *275*, 25089; e) R. Mitchell, A. J. Moddy, P. R. Rich, *Biochemistry* **1995**, *34*, 7576.
- [8] W. R. Scheidt, K. J. Haller, K. Hatano, *J. Am. Chem. Soc.* **1980**, *102*, 3017.
- [9] a) J. Li, B. C. Noll, C. E. Schulz, W. R. Scheidt, *Inorg. Chem.* **2007**, *46*, 2286; b) T. Ikeue, Y. Ohgo, T. Saitoh, M. Nakamura, H. Fujii, M. Yokoyama, *J. Am. Chem. Soc.* **2000**, *122*, 4068; c) A. Ikezaki, M. Nakamura, *Inorg. Chem.* **2002**, *41*, 2761.
- [10] W. R. Scheidt, C. A. Reed, *Chem. Rev.* **1981**, *81*, 543.
- [11] a) P. Gütllich, H. A. Goodwin, *Top. Curr. Chem.* **2004**, *233*, 1; b) P. Gütllich, P. J. van Koningsbruggen, F. Renz, *Struct. Bonding* **2004**, *107*, 27.
- [12] See the Supporting Information for computational details.
- [13] CCDC-699087, 699088, 699089, and 699090([K(222)][Fe-(tpp)(CN)] at 100, 296, 325 and 400 K) contain the supplementary crystallographic data for this paper. These data can be obtained free of charge from The Cambridge Crystallographic Data Centre via www.ccdc.cam.ac.uk/data_request/cif.
- [14] S. Neya, A. Takahashi, H. Ode, T. Hoshino, M. Hata, A. Ikezaki, Y. Ohgo, M. Takahashi, H. Hiramatsu, T. Kitagawa, Y. Furutani, H. Kandori, N. Funasaki, M. Nakamura, *Eur. J. Inorg. Chem.* **2007**, 3188.
- [15] J. J. Alexander, H. B. Gray, *J. Am. Chem. Soc.* **1968**, *90*, 4260.
- [16] F. A. Cotton, C. A. Murillo, M. Bochmann, *Advanced Inorganic Chemistry*, Wiley, New York, **1999**.
- [17] K. J. Nelson, I. D. Giles, W. W. Shum, A. M. Arif, J. S. Miller, *Angew. Chem.* **2005**, *117*, 3189; *Angew. Chem. Int. Ed.* **2005**, *44*, 3129.
- [18] a) R. J. Deeth, *Eur. J. Inorg. Chem.* **2006**, 2551; b) R. L. Lord, M.-H. Baik, *Inorg. Chem.* **2008**, *47*, 4413.
- [19] We have also synthesized and characterized six-coordinate cyanoferroporphyrinates; all are LS.